Single Image Ear Recognition Using Wavelet-Based Multi-Band PCA

Matthew Zarachoff
School of Computing, Creative Technologies & Engineering
Leeds Beckett University
Leeds, United Kingdom
m.zarachoff4868@student.leedsbeckett.ac.uk

Akbar Sheikh-Akbari
School of Computing, Creative Technologies & Engineering
Leeds Beckett University
Leeds, United Kingdom
A.Sheikh-Akbari@leedsbeckett.ac.uk

Dorothy Monekosso
School of Computing, Creative Technologies & Engineering
Leeds Beckett University
Leeds, United Kingdom
D.N.Monekosso@leedsbeckett.ac.uk

***Abstract*—Principal Component Analysis (PCA) has been successfully used for many applications, including ear recognition. This paper presents a 2D Wavelet based Multi-Band PCA (2D-WMBPCA) method, inspired by PCA based techniques for multispectral and hyperspectral images, which have shown a significantly higher performance to that of standard PCA. The proposed method performs 2D non-decimated wavelet transform on the input image dividing the image into its subbands. It then splits each resulting subband into a number of bands evenly based on the coefficient values. Standard PCA is then applied on each resulting set of bands to extract the subbands eigenvectors, which are used as features for matching. Experimental results on images of two benchmark ear image datasets show that the proposed 2D-WMBPCA significantly outperforms both the standard PCA method and the eigenfaces method.**

***Index Terms*—Ear recognition, principal component analysis, multi-band image creation, non-decimated wavelet transform**

I. Introduction

Ear recognition, a field within biometrics, concerns itself with the use of images of the ears to identify individuals. Much like fingerprints, ears are unique to an individual; even identical twins can have distinguishable ears [1]. Researchers have explored this topic extensively over the last two decades, investigating both the feature extraction and comparison of features of ear images [2], [3]. Successful feature extraction techniques in ear recognition include Principal Component Analysis (PCA) [2], [4]–[7], wavelet based [8], and neural network based methods [9]–[11]. Amongst these techniques, PCA has been found to be successful for both feature extraction [4]–[6] and feature reduction to reduce dimensionality of the data [2], [3]. In general, PCA based techniques operate by converting an image into a 1D vector and concatenating those vectors to form a 2D matrix. While some PCA based ear recognition techniques have been reported in the literature [2], [4], [5], [12], these techniques involve projecting ear images into a common eigenspace. In contrast, the authors previously introduced a single image PCA based technique for ear recognition in [13], inspired by hyperspectral PCA based techniques [14] such as Segmented PCA [15] and Folded PCA [16], which solely use the extracted principal components as features. To the authors' knowledge, no similar techniques that utilize wavelets have been reported in the literature. This has inspired the authors to propose a single image, PCA based method for ear recognition, called 2D Wavelet based Multi-Band PCA (2D-WMBPCA). Unlike the aforementioned PCA based methods, the proposed technique does not require the images to be projected into a common eigenspace. Instead, the proposed technique performs a 2D non-decimated wavelet transform on the input image, dividing the image into its subbands. The resulting subbands are then split evenly into a number of bands according to their their coefficient values.The proposed technique then applies the standard PCA method on each resulting set of bands to extract their principal components as their features that are then used for recognition. Experimental results on the images of two benchmark ear image datasets demonstrate that the proposed 2D-WMBPCA technique greatly outperforms both single image PCA and the eigenfaces technique. The rest of the paper is organized as follows: Section II introduces the proposed 2D-WMBPCA technique, Section III describes the benchmark datasets used, Section IV discusses the experimental results, and finally Section V concludes the paper.

II. Proposed 2D-WMBPCA Method

The proposed 2D Wavelet based Multi-Band Principal Component Analysis (2D-WMBPCA) method includes the following five stages: Wavelet Decomposition, Pre-processing, Multiple-image generation, PCA, and Eigenvector matching. Fig. 1 shows the block diagram of the proposed 2D-WMBPCA technique.

A. Wavelet Decomposition

Let E be the set of all ear images, where each input image $e \in E$ is an 8-bit, grayscale image. The proposed technique performs a 2D non-decimated discrete dyadic wavelet transform on the input image, e, using the non-orthogonal wavelet and the fast computation algorithm introduced by Mallat and Hwang in [17], splitting the input image into its four subbands called: Low-Low (LL), Low-High (LH), High-Low (HL), and High-High (HH).

B. Pre-processing

Coefficients within each subband s are then mapped to the [0, 1] domain using (1):

978-9-0827-9703-9/19/$31.00 ©2019 IEEE

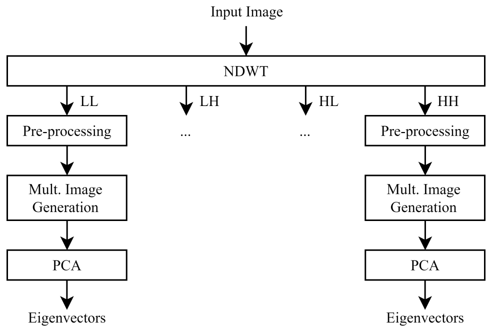

Fig. 1. Block diagram of the proposed 2D-WMBPCA method.

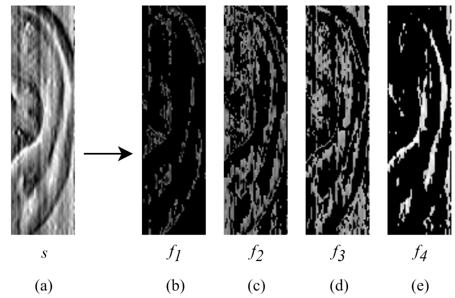

Fig. 2. An example of multiple image generation: a) Pre-processed input subband s from an image in the IITD II dataset [18], resulting multiple bands b) f_1 c) f_2 d) f_3 e) f_4. The coefficients for images b) and c) have been multiplied by 1.5 and 1.25 respectively for illustration purposes.

$$p' = \frac{p - min(s)}{max(s) - min(s)} \tag{1}$$

where p represents an original coefficient in s and p' represents the corresponding mapped coefficient.

Histogram equalization is then performed on the resulting subband coefficients to increase their contrast. To do so, the Probability Mass Function (PMF) of the resulting subbands coefficients is first calculated using (2):

$$P_X(x_k) = P(X = x_k) \text{ for } k = 0, 1, ..., 255 \tag{2}$$

where $X = x_1, x_2, ..., x_k$ represent the subbands' coefficients and $P_X(x_k)$ is the probability of coefficients in bin k. The resulting PDF is then used to calculate the Cumulative Distribution Function (CDF) of the subband using (3):

$$C_X(k) = P(X \leq x_k) \text{ for } k = 0, 1, ..., 255 \tag{3}$$

where $C_X(k)$ is the cumulative probability of $X \leq x_k$. Finally, all subbands coefficients are mapped to new values using the resulting CDFs. This improves the contrast of the subbands coefficients.

C. Multiple-Image Generation

Various methods can be used by proposed 2D Wavelet based Multi-Band PCA (2D-WMBPCA) to generate multiple bands from each input histogram equalized subband. The multiple band generation method used in this research can be formulated as follows:

Assume s is the input subband and N is the number of desired bands to be generated from the subband s. The proposed algorithm uses $N - 1$ boundaries to split the input subbands coefficients into N target bands according to the coefficient values. Let $B = [b_1, b_2, ..., b_{N-1}]$ be the boundary values, calculated according to (4):

$$b_n = n/N \text{ for } n = 1, ..., (N - 1) \tag{4}$$

The input subband s coefficients are divided into N target bands as follows:

1) Generate N images of the same size of s and set their coefficients to zero. These bands are called: $F = [f_1, f_2, ..., f_N]$
2) Split the input subbands coefficients into different bands according to their values using the following ranges: $[0, b_1), [b_1, b_2), ..., [b_{N-1}, 1]$

It generates F bands from input subband, where these bands, in a sense, form a multispectral image. An illustration of the process to generate four bands can be seen in Fig. 2.

D. Principal Component Analysis

Assume F is the set of resulting bands and $F = [f_1, f_2, ..., f_N]$. For each band $f \in F$, a mean adjusted image f' is created using (5):

$$f' = f - \overline{f} \tag{5}$$

where $\overline{f}$ is the mean value of the coefficients in f. Every band is then converted to a column wise vector, allowing F to be represented as a two dimensional matrix W. PCA is then performed using Singular Value Decomposition (SVD) on matrix W, creating the decomposition in (6):

$$W = U\Sigma V^T \tag{6}$$

where U is a unitary matrix and the columns of V are the orthonormal eigenvectors of the covariance matrix of W and Σ is a diagonal matrix of their respective eigenvalues. The eigenvectors form a basis for an eigenspace for each set of images F. The resulting principal components in V are finally used for matching.

E. Subband Matching

Let $M = [m_1, m_2, ..., m_{N-1}]$ be the set of principal components of a query image subband q. Furthermore, let $L = [l_1, l_2, ..., l_{N-1}]$ be the set of principal components of subband r, a subband of an image in the image dataset. The set of Euclidean distances $D = [d_1, d_2, ..., d_{N-1}]$ between q and r can be calculated using (7):

$$d_n = \sqrt{(\Sigma_n (m_n - l_n)^2)} \tag{7}$$

The resulting Euclidean distances are summed to produce the total distance between the two subbands. The resulting differences across all four subbands (LL, LH, HL, HH) are then summed to produce the total distance between the two images. The best match for query image q in the image database is the image for which the total distance is minimized.

III. Benchmark Datasets

This investigation uses two benchmark ear image datasets: The Indian Institute of Technology Delhi II (IITD II) dataset [18] and the University of Science and Technology Beijing I (USTB I) dataset 5 [19]. IITD II dataset consists of 793 images of the right ear of 221 participants. Each participant was photographed between three and six times, with each image being of size 180 $\times$ 50 pixels and in 8-bit grayscale. For consistency, only the first three images for each individual are used in this research. The USTB I dataset consists of 180 images of the right ear of 60 participants, each of whom were photographed three times. The images of this dataset are 8-bit grayscale of size 150 $\times$ 80 and are tightly cropped; however, some of the images exhibit slight yaw and shearing.

IV. Experimental Results

To assess the performance of the proposed 2D Wavelet based Multi-Band PCA (2D-WMBPCA) technique and compare its performance against standard Principal Component Analysis (PCA) method for ear recognition, the aforementioned two ear image datasets were used. The proposed 2D-WMBPCA method using the two boundary selection algorithms described in Section III and the standard PCA method were applied to the images of the two datasets. All of the experiments began by selecting the first image of each subject to serve as a query set and the rest of the images to be a dataset. Given a particular query image, if it is correctly matched with an image in the dataset, it is marked as a Top-1 image. Similarly, if it is correctly matched with any of the closest five images, it is marked as a Top-5 image. The percentage of Top-1 and Top-5 images in the dataset are then listed as Top-1 and Top-5 accuracies. Finally, this process is repeated for the second and third images for each individual, with the Top-1 and Top-5 accuracies averaged across all trials.

A. *Experimental Results for the Standard PCA Method*

To create results for the standard PCA method, the PCA was applied to each original image individually. Their resulting eigenvectors were then compared using Euclidean distance. The results for the application of PCA on the images of the IITD II and USTB I datasets are presented in Table I. From Table I, it can be seen that the performance of PCA on the images of the IITD II dataset is lower than than that of the USTB I dataset. This can be explained by the fact that some of the IITD IIs images have a slight yaw, which causes slight occlusion.

TABLE I
Experimental Results for Standard PCA (%)

Dataset	**Type of Match**	
	Top-1	***Top-5***
IITD II	36.35	52.94
USTB I	45.00	70.00

TABLE II
Experimental results for the Eigenfaces PCA method (%)

Dataset	**Type of Match**	
	Top-1	***Top-5***
IITD II	89.78	95.64
USTB I	75.93	90.74

B. *Experimental Results for the Eigenfaces Method*

To generate experimental results for the PCA based eigenfaces method [5], 10% of images of each ear dataset were used to calculate the eigenvectors. The remaining images were then projected along the resulting eigenvectors to create eigenears, which were compared using the Euclidean distance. The experimental results are tabulated in Table II. From Table II, it can be seen that the eigenfaces method vastly outperforms single image PCA on the images of the both the IITD II and USTB I datasets. Interestingly, however, the eigenfaces method achieves higher accuracy on the images of IITD II dataset. This could be attributed to the wider diversity of ear images which IITD II contains compared to the images within the USTB I dataset.

C. *Experimental Results for the Proposed 2D-WMBPCA Method*

The proposed 2D-WMBPCA method was applied to both images of the IITD II and USTB I datasets using two to twenty bands of constant size, as discussed in Section III. The number of correct matches was calculated for each set of bands. A subset of the results for both the IITD II and USTB I image datasets are tabulated in Table III.

From Table III, it can be seen that the proposed 2D-WMBPCA method significantly outperforms the standard PCA method on images of both the IITD II and USTB I datasets. From Table I and II, it is evident that the Top-1 accuracy of matching has been improved by 57.79% and 51.30% on the images of the IITD II dataset using three bins and images of the USTB I dataset using four bins when compared to standard PCA, respectively. Furthermore, the Top-1 accuracy for 2D-MBPCA on the IITD II and USTB I datasets increased by 4.36% and 20.37% when compared to eigenfaces, respectively. From the experiments presented in these two tables, it can be seen that the proposed 2D-WMBPCA method achieves its highest performance when using just three/four bands.

To compare the performance of the proposed technique with the state of the art PCA and learning based techniques, the Top-1 experimental results of the proposed 2D-CMBPCA, single image PCA, eigenfaces [5], 2D-MBPCA [13], BSIF

TABLE III
EXPERIMENTAL RESULTS FOR THE PROPOSED TECHNIQUE ON THE IITD II DATASET [18] (%)

Type of Match		Number of Bands
Top-1	***Top-5***	
90.28	94.64	2
94.14	**97.49**	3
92.80	97.32	4

TABLE IV
EXPERIMENTAL RESULTS FOR THE PROPOSED TECHNIQUE ON THE USTB I DATASET [19] (%)

Type of Match		Number of Bands
Top-1	***Top-5***	
93.83	97.53	3
96.30	**98.15**	**4**
96.30	**98.15**	**5**
94.44	98.15	6

TABLE V
TOP-1 RESULTS FOR THE PROPOSED TECHNIQUE AND OTHER PCA AND LEARNING BASED TECHNIQUES (%)

Algorithm	Dataset	
	IITD II	***USTB I***
PCA based Techniques		
Single Image PCA	36.35	45.00
Eigenfaces [5]	89.78	75.93
2D-MBPCA [13]	92.76	96.11
Proposed Technique	**94.14**	**96.30**
Learning based Techniques		
BSIF and SVM [20]	97.31	-
Neural Network and SVM [9]	-	98.30

[20], and neural network and SVM based [9] techniques are tabulated in Table V. From Table V, it can be noted that the proposed 2D-WMBPCA technique significantly outperforms the single image PCA, eigenfaces, and 2D-MBPCA methods. Furthermore, the proposed method gives competitive results compared to learning based techniques.

V. CONCLUSION

In this paper, a non-decimated wavelet and PCA based ear recognition algorithm, called 2D Wavelet based Multi-Band PCA (2D-WMBPCA), was presented. Experimental results on the images of two benchmark ear image datasets show that the proposed 2D-WMBPCA technique significantly outperforms both the standard PCA, eigenfaces, and 2D-MBPCA methods. Furthermore, it generates competitive results to those of the state of the art learning based techniques.

REFERENCES

[1] H. Nejati, L. Zhang, T. Sim, E. Martinez-Marroquin, and G. Dong, “Wonder ears: Identification of identical twins from ear images,” in *Proceedings of the 21st International Conference on Pattern Recognition (ICPR2012)*, Nov. 2012, pp. 1201–1204.

[2] v. Emeršič, V. Štruc, and P. Peer, “Ear recognition: More than a survey,” *Neurocomputing*, vol. 255, pp. 26–39, Sep. 2017. [Online]. Available: http://linkinghub.elsevier.com/retrieve/pii/S092523121730543X

[3] A. Pflug and C. Busch, “Ear biometrics: a survey of detection, feature extraction and recognition methods,” *IET Biometrics*, vol. 1, no. 2, pp. 114–129, Jun. 2012.

[4] B. Victor, K. Bowyer, and S. Sarkar, “An evaluation of face and ear biometrics,” in *Object recognition supported by user interaction for service robots*, vol. 1, 2002, pp. 429–432 vol.1.

[5] K. Chang, K. W. Bowyer, S. Sarkar, and B. Victor, “Comparison and combination of ear and face images in appearance-based biometrics,” *IEEE Transactions on Pattern Analysis and Machine Intelligence*, vol. 25, no. 9, pp. 1160–1165, Sep. 2003.

[6] D. Querencias-Uceta, B. Ríos-Sánchez, and C. Sánchez-Ávila, “Principal component analysis for ear-based biometric verification,” in *2017 International Carnahan Conference on Security Technology (ICCST)*, Oct. 2017, pp. 1–6.

[7] M. A. Turk and A. P. Pentland, “Face recognition using eigenfaces,” in *1991 IEEE Computer Society Conference on Computer Vision and Pattern Recognition Proceedings*, Jun. 1991, pp. 586–591.

[8] M. S. Nosrati, K. Faez, and F. Faradji, “Using 2d wavelet and principal component analysis for personal identification based On 2d ear structure,” in *2007 International Conference on Intelligent and Advanced Systems*, Nov. 2007, pp. 616–620.

[9] I. Omara, X. Wu, H. Zhang, Y. Du, and W. Zuo, “Learning pairwise SVM on deep features for ear recognition,” in *2017 IEEE/ACIS 16th International Conference on Computer and Information Science (ICIS)*, May 2017, pp. 341–346.

[10] F. I. Eyiokur, D. Yaman, and H. K. Ekenel, “Domain adaptation for ear recognition using deep convolutional neural networks,” *IET Biometrics*, vol. 7, no. 3, pp. 199–206, 2018.

[11] S. Dodge, J. Mounsef, and L. Karam, “Unconstrained ear recognition using deep neural networks,” *IET Biometrics*, vol. 7, no. 3, pp. 207–214, 2018.

[12] J. Yang, D. Zhang, A. F. Frangi, and J.-y. Yang, “Two-dimensional PCA: a new approach to appearance-based face representation and recognition,” *IEEE Transactions on Pattern Analysis and Machine Intelligence*, vol. 26, no. 1, pp. 131–137, Jan. 2004.

[13] M. Zarachoff, A. Sheikh-Akbari, and D. Monekosso, “2d Multi-Band PCA and its Application for Ear Recognition,” in *2018 IEEE International Conference on Imaging Systems and Techniques (IST)*, Oct. 2018, pp. 1–5.

[14] J. C. Harsanyi and C. I. Chang, “Hyperspectral image classification and dimensionality reduction: an orthogonal subspace projection approach,” *IEEE Transactions on Geoscience and Remote Sensing*, vol. 32, no. 4, pp. 779–785, Jul. 1994.

[15] X. Jia and J. A. Richards, “Segmented principal components transformation for efficient hyperspectral remote-sensing image display and classification,” *IEEE Transactions on Geoscience and Remote Sensing*, vol. 37, no. 1, pp. 538–542, Jan. 1999.

[16] J. Zabalza, J. Ren, M. Yang, Y. Zhang, J. Wang, S. Marshall, and J. Han, “Novel Folded-PCA for improved feature extraction and data reduction with hyperspectral imaging and SAR in remote sensing,” *ISPRS Journal of Photogrammetry and Remote Sensing*, vol. 93, pp. 112–122, Jul. 2014. [Online]. Available: http://www.sciencedirect.com/science/article/pii/S0924271614000938

[17] S. Mallat and W. L. Hwang, “Singularity detection and processing with wavelets,” *IEEE Transactions on Information Theory*, vol. 38, no. 2, pp. 617–643, Mar. 1992.

[18] “IIT Delhi Ear Database.” [Online]. Available: http://www4.comp.polyu.edu.hk/csajaykr/IITD/Database_Ear.htm

[19] “Ear Recoginition Laboratory at USTB.” [Online]. Available: http://www1.ustb.edu.cn/resb/en/index.htm

[20] A. Benzaoui, N. Hezil, and A. Boukrouche, “Identity recognition based on the external shape of the human ear,” in *2015 International Conference on Applied Research in Computer Science and Engineering (ICAR)*, Oct. 2015, pp. 1–5.